AJNR

Myelographic Techniques for the Localization of CSF-Venous Fistulas: Updates in 2024

Ajay A. Madhavan, Waleed Brinjikji, Jeremy K. Cutsforth-Gregory, Timothy J. Amrhein, Peter G. Kranz, John C. Benson, Felix E. Diehn, Ben A. Johnson-Tesch, Greta B. Liebo, Vance T. Lehman, Ian T. Mark, Pearse P. Morris, Michael P. Oien, Darya P. Shlapak and Jared T. Verdoorn

Myelographic Techniques for the Localization of CSF-Venous Fistulas: Updates in 2024

Ajay A. Madhavan, Waleed Brinjikji, Jeremy K. Cutsforth-Gregory, Timothy J. Amrhein, Peter G. Kranz, John C. Benson, Felix E. Diehn, Ben A. Johnson-Tesch, Greta B. Liebo, Vance T. Lehman, Ian T. Mark, Pearse P. Morris, Michael P. Oien, Darya P. Shlapak, and Jared T. Verdoorn

ABSTRACT

SUMMARY: CSF-venous fistulas (CVFs) are a common cause of spontaneous intracranial hypotension. Despite their relatively frequent occurrence, they can be exceedingly difficult to detect on imaging. Since the initial description of CVFs in 2014, the recognition and diagnosis of this type of CSF leak has continually increased. As a result of multi-institutional efforts, a wide spectrum of imaging modalities and specialized techniques for CVF detection is now available. It is important for radiologists to be familiar with the multitude of available techniques, because each has unique advantages and drawbacks. In this article, we review the spectrum of imaging modalities available for the detection of CVFs, explain the advantages and disadvantages of each, provide typical imaging examples, and discuss provocative maneuvers that may improve the conspicuity of CVFs. Discussed modalities include conventional CT myelography, dynamic myelography, digital subtraction myelography, conebeam CT myelography, decubitus CT myelography by using conventional energy-integrating detector scanners, decubitus photon counting CT myelography, and intrathecal gadolinium MR myelography. Additional topics to be discussed include optimal patient positioning, respiratory techniques, and intrathecal pressure augmentation.

ABBREVIATIONS: AP = anteroposterior; CBCT = conebeam CT; CB-CTM = conebeam CT myelography; CTM = CT myelography; CVF = CSF-venous fistula; DSM = digital subtraction myelography; EID = energy-integrating detector; GdM = intrathecal gadolinium MR myelography; IVVP = internal vertebral venous plexus; PCCT = photon-counting detector CT; PC-CTM = photon-counting CT myelography; SIH = spontaneous intracranial hypotension; SR = standard resolution; UHR = ultra-high resolution; VMI = virtual monoenergetic image

Spontaneous intracranial hypotension (SIH) is caused by a CSF leak in the spine.[1] Although the hallmark symptom of SIH is an orthostatic headache, a wide variety of symptoms can occur. Clinical manifestations of SIH are frequently debilitating and occasionally life-threatening.[2] Currently, 3 main types of spinal CSF leaks are recognized. These include dural tears (type 1a ventral, type 1b posterolateral), leaking meningeal diverticula (type 2), and CSF-venous fistulas (CVFs; type 3).[1] Patients with any type of spinal CSF leak may present with characteristic abnormalities on brain MR imaging, which can predict the probability of localizing a CSF leak on subsequent testing.[3,4] However, some patients with SIH have normal brain MR imaging.[5]

Although each leak type presents its own challenges for diagnosis, CVFs can be particularly elusive for several reasons. First, patients with CVFs almost never harbor extradural CSF on spine imaging (neither MR imaging nor CT myelography).[6] Indeed, some patients with CVFs have almost entirely normal brain and spine MR imaging, although spine imaging does usually demonstrate the presence of meningeal diverticula.[5] As a result, the diagnosis of SIH is overlooked in some patients. Second, CVFs usually require advanced myelographic techniques for detection, necessitating technology that is not ubiquitously available. Some patients, therefore, may experience delayed diagnosis.[7] Finally, CVFs are likely intermittent in nature. Therefore, a single negative high-quality myelogram does not necessarily exclude the presence of a CVF, compounding an already challenging scenario.[8,9]

Since the initial description of CVFs in 2014, substantial progress has been made to improve their detection, and extensive information about this topic has been published.[10] Today, a wide variety of myelographic techniques for the detection of CVFs is available.[11] It is important for radiologists, particularly those performing advanced myelography, to be aware of established and emerging techniques, understand how to perform them optimally, and be familiar with the advantages and disadvantages of each. In this review, we discuss conventional CT myelography (CTM), dynamic fluoroscopic myelography, digital subtraction myelography (DSM), decubitus CTM on energy-integrating
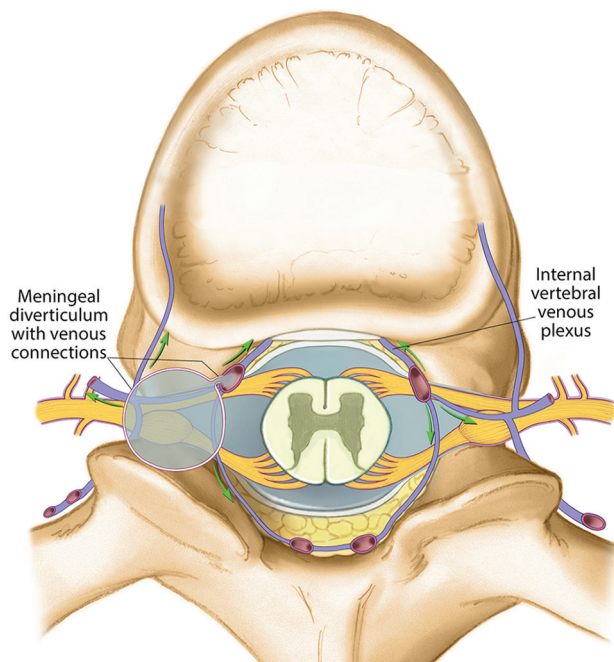
FIG 1. Illustration of the venous anatomy relevant to CVF imaging. CVFs most commonly arise in association with meningeal diverticula. The internal vertebral venous plexus is an often overlooked drainage pathway that can be particularly subtle on imaging.

detector (EID) scanners, conebeam CT myelography (CB-CTM), photon-counting CTM (PC-CTM), and intrathecal gadolinium MR myelography (GdM). Additionally, we discuss provocative maneuvers that may improve the conspicuity of CVFs.

GENERAL PRINCIPLES

CVFs are abnormal connections between the subarachnoid space and the venous system leading to unregulated loss of CSF volume, ultimately causing SIH.[12] The precise mechanism of CVF development is unknown, with leading theories suggesting that spinal arachnoid granulations and/or sequelae of minor dural trauma may play a role.[13-15] CVFs are more common in patients with a higher than average body mass index, and it is likely that some CVFs originate as a result of intracranial hypertension.[16] The reported age ranges for patients with CVFs varies, with 1 study suggesting a mean age of 53 years and a range of 33–72 years.[17] Although data regarding the frequency of CVFs are lacking, some studies suggest that CVFs account for as many as 50% of cases of SIH.[18]

Most CVFs occur in the thoracic spine.[11] However, cervical, lumbar, and sacral CVFs have also been described.[19] At least 1 case of a skull base CVF has been reported, although this was secondary to major trauma.[20] Almost all CVFs arise from the lateral portions of the thecal sac, usually but not always in association with nerve root sleeve/meningeal diverticula. Most studies have shown that CVFs are more common on the right side; therefore, advanced myelography searching for a right-sided CVF is usually performed before studying the left side.[12] CVFs may drain into any number of a complex network of veins in the spine (Fig 1). Generally, these can be divided into the internal vertebral venous

plexus (IVVP or internal epidural venous plexus), the external vertebral venous plexus (consisting of the paraspinal segmental vein, lateral/intercostal branches, and posterior muscular branches), and the basivertebral venous plexus.[12] Regardless of the imaging technique used to detect CVFs, understanding this anatomy is critical to refining one's search pattern for locating leaks. On rare occasions, CVFs may be associated with paraspinal venous malformations, and this may account for an increased incidence of SIH in patients with Klippel-Trenaunay syndrome.[21-24] A similar phenomenon can also be seen with paraspinal lymphatic malformations.[25]

IMAGING MODALITIES FOR CVF DETECTION
Conventional CT Myelography
No consistent definition of "conventional" CTM exists in the literature. However, in general terms, we consider conventional CTM to consist of a supine or prone CT myelogram that is obtained in a delayed fashion (more than approximately 15 minutes) after injection of intrathecal contrast.[26] At most institutions, contrast injection is performed under fluoroscopic guidance in the prone or decubitus position. Before the delayed CT myelogram, the patient is usually rolled several times to allow contrast to distribute evenly throughout the subarachnoid space.

Conventional CTM is excellent for anatomic evaluation of the intrathecal and adjacent structures, characterization of spondylotic changes, and detection of extradural CSF. However, it is suboptimal for the localization of CVFs for 2 main reasons.[27] First, because most CVFs arise from meningeal diverticula, it is necessary to have high-attenuation contrast in the pathologic nerve root sleeve to maximize the attenuation of the draining vein. Due to the relatively low concentration of intrathecal contrast on conventional CTM, which has been diluted throughout the subarachnoid space, draining veins are frequently occult. Second, studies with dynamic imaging have shown that CVFs are sometimes most apparent within the first seconds to minutes after intrathecal contrast injection. Therefore, some CVFs may not be visible given the delayed timing inherent in conventional CTM.

In some cases, however, CVFs can be seen on conventional CTM. Even if a definitive CVF is not localized, subtle or equivocal imaging findings may be helpful to direct subsequent imaging studies (Fig 2). Although we do not routinely recommend the use of conventional CTM for the diagnosis of CVFs, patients may present having already had 1 or more such studies. Thus, we still encourage scrutiny of any available conventional CTMs before performing additional myelography. Importantly, conventional CTM can falsely localize or otherwise misrepresent the presence of a CVF, and follow-up decubitus myelography is generally recommended to confirm findings.

Dynamic Myelography and DSM
Dynamic myelography refers to a fluoroscopic myelogram by using real-time imaging with a high frame rate (typically 0.5–2 frames per second).[28] Usually, dynamic myelography is performed with the patient in the Trendelenburg position to promote caudocranial contrast flow. This can be achieved with a tilting fluoroscopy table, a wedge or other device placed under the patient's pelvis, or some combination of the two. This technique permits

real-time visualization of CVFs as contrast opacifies and exits draining veins (Fig 2). DSM refers to essentially the same technique, except that digital subtraction is used to help distinguish contrast from other high-density structures such as the vertebral elements (Fig 3). DSM was initially performed in the prone position for the localization of ventral dural tears.[29] The first reported CVFs were detected incidentally on prone DSM.[10] Later, it was found that lateral decubitus DSM increased the diagnostic yield for CVF detection.[30]

Although both dynamic myelography and DSM are excellent modalities for CVF detection, the latter is generally preferred to maximize the sensitivity of the examination. Precise technique varies among different institutions. Dynamic myelography and DSM can be performed under general anesthesia to eliminate respiratory motion during imaging, but diagnostic images can often be obtained in awake or moderately sedated patients. Patients should always be in the decubitus position to maximize the sensitivity of the examination. Single anteroposterior (AP) plane or biplane (AP and lateral) imaging can be done. Typically, 2 separate acquisitions lasting approximately 60 seconds are performed, with the first centered over the lower cervical/upper thoracic spine and the second centered over lower thoracic/upper lumbar spine. During each acquisition, 5–6 mL of iodinated contrast (iohexol 300 mg/mL such as Omnipaque 300, GE Healthcare) are injected. The use of lower concentration iohexol formulations (such as Omnipaque 240) is generally not advisable due to suboptimal visualization of contrast.
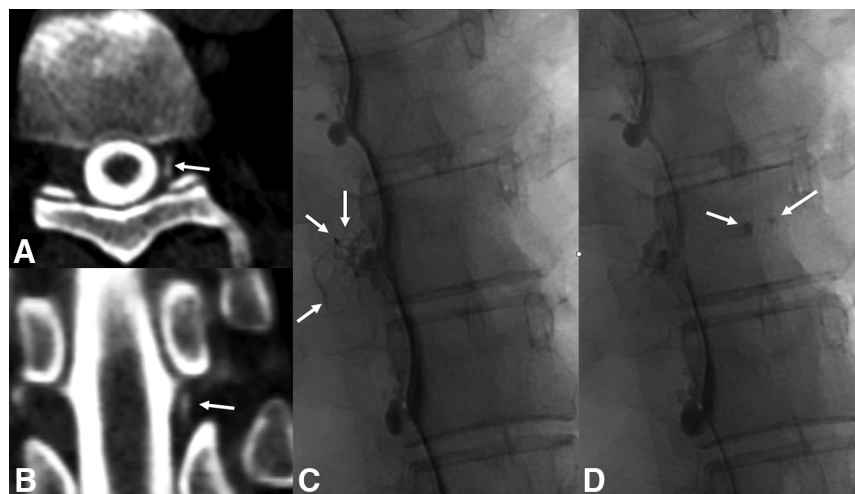

FIG 2. CVFs seen on conventional CT myelography and dynamic fluoroscopic myelography. Axial (*A*) and coronal (*B*) images from a conventional supine CT myelogram demonstrate subtle opacification of the internal epidural venous plexus (*A and B, arrow*), compatible with a CVF, which was subsequently confirmed on decubitus digital subtraction myelography (not shown). In a different patient, 2 AP images spaced 20 seconds apart from a left lateral decubitus dynamic myelogram (*C and D*) demonstrate a left T8 CVF involving several paraspinal veins (*C, arrows*), as well as the basivertebral venous plexus (*D, arrows*). The temporal resolution conferred by dynamic myelography is helpful to characterize the full extent of venous drainage.

Summary of imaging modalities available to detect CVFs

| Imaging Technique	Advantages	Disadvantages	Relative Diagnostic Yield for CVF	Relative Radiation Dose	Availability
Conventional CTM	Detects extradural CSF; sometimes identifies slow leaks	No temporal resolution	Low	+	Widely available
Dynamic myelography and DSM	High spatial and temporal resolution	No cross-sectional detail, usually requires 2 days	High	+	Intermediate availability (requires high-quality interventional suite)
Conebeam CTM	High spatial resolution; cross-sectional	Small FOV	High	+	Intermediate availability (requires high-quality interventional suite)
EID CTM	Cross-sectional; some temporal resolution if dynamic; can be done in single day	Less spatial/temporal resolution than DSM	High	+++	Widely available
PC-CTM	Cross-sectional; high spatial and temporal resolution; spectral information; can be done in single day	Less temporal resolution than DSM	Very high	++	Low availability
GdM	Cross-sectional; detects extradural CSF and sometimes slow leaks	Less spatial/temporal resolution compared with other techniques; off-label use of gadolinium; flow artifacts	Low	none	Widely available
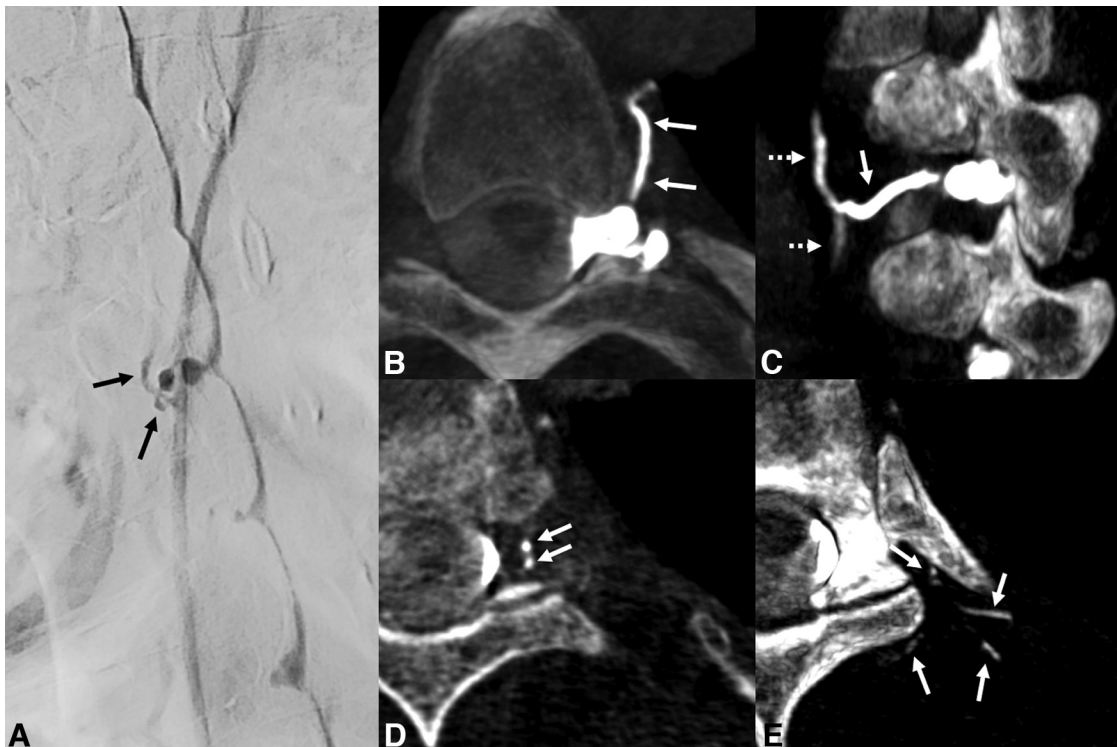
FIG 3. Left T4 CSF-venous fistula seen on digital subtraction myelography and CB-CTM. Left lateral decubitus digital subtraction myelogram (*A*) demonstrates curvilinear venous opacification adjacent to a left T4 diverticulum (*A*, *arrows*), compatible with a CVF. High-resolution CBCT was performed next after centering the flat panel detector over the level of T4, with imaging performed during active injection of 4 mL Omnipaque 300. Axial (*B*, *D*, and *E*) and sagittal (*C*) reformatted CBCT images demonstrate a definitive left T4 CVF involving the paraspinal segmental vein (*B and C*, *arrows*), the hemiazygous vein (*C*, *dashed arrows*), the internal epidural venous plexus (*D*, *arrows*), and small lateral and paraspinal muscular venous branches (*E*, *arrows*).

Dynamic myelography and DSM have many advantages that make them excellent for CVF detection. Because they are fluoroscopic modalities, they have higher spatial and temporal resolution than any CT- or MR imaging–based technique. The main disadvantage is the lack of cross-sectional detail. Biplane fluoroscopy can mitigate this limitation, but obtaining a diagnostic lateral view can be challenging in larger patients, especially near the cervicothoracic junction. Furthermore, both AP and lateral views can often be degraded by respiratory or other motion artifacts if general anesthesia is not used. DSM and dynamic myelography usually must be performed over 2 days, because the maximum recommended dose of intrathecal iodine (3 g, or 10 mL Omnipaque 300) is typically needed to study each side. While 5 mL of contrast is usually sufficient to coat the lateral thecal sac, dynamic myelography and DSM require 2 injections because the entire spine cannot be imaged in each acquisition. Notably, the daily contrast dose of 10 mL can often be safely exceeded by at least 50%, sometimes allowing a single-day bilateral dynamic myelogram or DSM. Nonetheless, DSM has a high diagnostic yield, exceeding 50% in most studies (although variable in different patient populations).[30,31]

Conebeam CT Myelography
CB-CTM refers to the use of a rotating flat panel x-ray detector to provide cross-sectional imaging. Unlike traditional CT, conebeam CT (CBCT) uses a cone-shaped x-ray source that covers the entire FOV in a single rotation. Many modern fluoroscopy systems have CBCT capabilities with various settings to modulate the frame rate, degrees of rotation, and other parameters to balance image quality with radiation dose. CB-CTM was recently described as an adjunct to DSM, localizing some CVFs that were undetectable on the initial DSM.[32]

One major advantage of CB-CTM is that it provides high spatial resolution, which is typically greater than that provided by most traditional CT scanners.[33] Furthermore, CB-CTM can be done during real-time fluoroscopic visualization of injected contrast. Thus, images can be obtained as soon as intrathecal contrast reaches the spinal level of greatest interest. The main disadvantage of CB-CTM is that the FOV is limited to approximately 6 vertebral levels.[32] It is often, therefore, best used as a problem-solving tool for equivocal findings on DSM. Even in cases in which a definitive CVF is seen on DSM, CB-CTM can be performed immediately afterward to provide anatomic characterization of venous drainage, which is helpful for treatment planning (Fig 3). The use of CB-CTM in addition to DSM is promising, although further study is needed to determine its added value.

Decubitus EID CT Myelography
Although CVFs were initially described and investigated by using DSM, decubitus CTM is also a highly effective technique for CVF
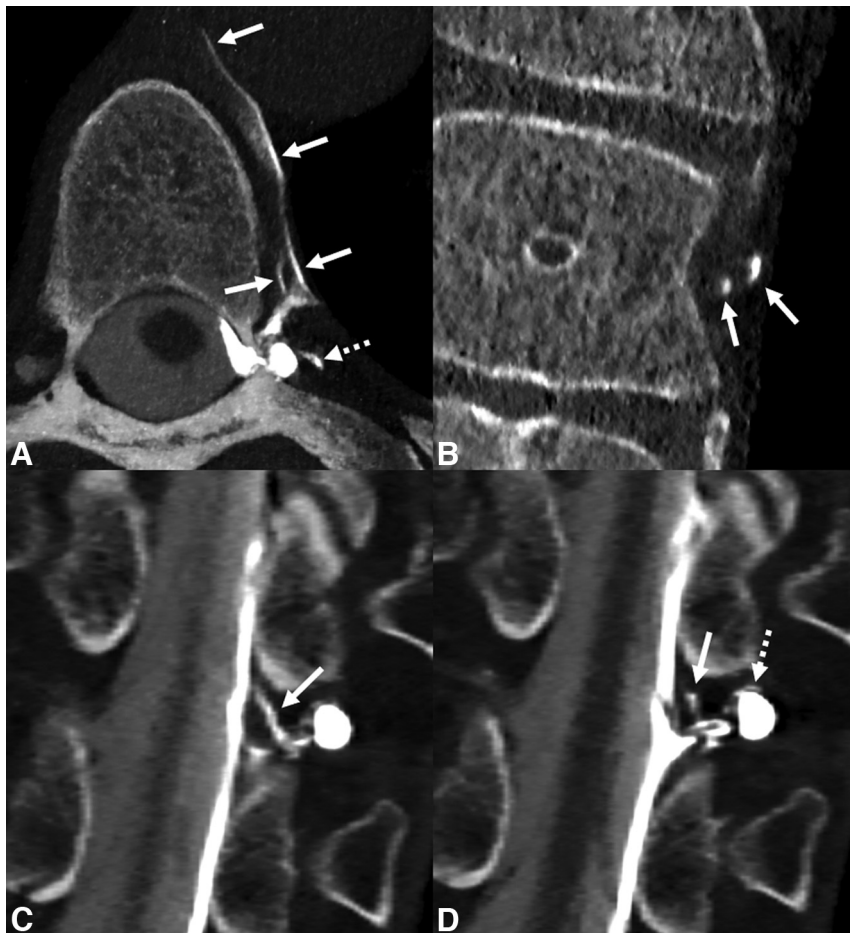
FIG 4. Typical appearance of CVFs on single-day bilateral decubitus CTM in 2 different patients (*A and B* versus *C and D*). In both patients, right lateral decubitus CTM was performed initially with injection of 5 mL Omnipaque 300 (not shown). Subsequently, the spinal needle was removed, the patients were rotated to the left decubitus position, and myelography was repeated with another 5 mL Omnipaque 300 after placement of a new spinal needle. In the first patient, axial (*A*) and coronal (*B*) images demonstrate a left T7 CVF involving the paraspinal segmental vein (*A and B, solid arrows*) and a lateral venous branch (*A, dashed arrow*). In the second patient, whose myelogram was performed on photon-counting CT, coronal 0.2 mm images (*C and D*) demonstrate a left T10 CVF involving the internal epidural venous plexus (*C and D, solid arrows*) and the intervertebral vein (*D, dashed arrow*). Detection of venous opacification immediately adjacent to meningeal diverticula often requires high spatial resolution.

detection.[34] Decubitus CTM is performed on a variety of EID CT scanners, including those with dual-energy capabilities. Decubitus CTM can be done by using a single CT acquisition of the spine, or it can be performed in a dynamic fashion using multiple, successive scans to confer temporal resolution. The added value of dynamic CTM for improving CVF detection rate has been described previously.[35]

To our knowledge, no currently available modern generation CT scanners have tilting table capabilities. Therefore, decubitus CTM requires an external device to elevate the pelvis and promote caudocranial contrast flow. This can be accomplished with a custom wedge, inflatable devices, or a recently introduced hand-operated elevation device.[36] If an accurate CSF opening pressure is desired, this must be obtained before elevation of the pelvis to avoid a spuriously low CSF pressure reading. With consistent pelvic elevation of 10°–15°, contrast usually reaches the cervical spine in 10–20 seconds. In patients with scoliosis, contrast can take variable amounts of time to ascend from the lumbar to cervical spine, and real-time fluoroscopy is not available as it is with DSM. This can make it challenging to achieve optimal scan timing after contrast injection. However, bolus tracking by using low-dose monitoring scans can be used to accurately gauge the ascent of intrathecal contrast, preventing premature scanning and unnecessary radiation.[37]

Although there is no single best accepted imaging reconstruction protocol for decubitus CTM, certain key concepts should be followed. First, thin-section imaging is critical to identify CVFs. This is because thicker slices result in volume averaging of opacified veins, obscuring important findings. Generally, a submillimeter section thickness is necessary.[17] Second, sharper kernel reconstructions may be helpful to improve spatial resolution.[38] However, this comes at the cost of increased noise, and a balance between resolution and SNR must be achieved. Finally, dual-energy CT may be helpful to increase conspicuity of subtle CVFs. Reconstruction of virtual monoenergetic images (VMIs) at 40–60 keV is optimal for this purpose.[39]

The primary advantage offered by decubitus CTM over dynamic fluoroscopic myelography and DSM is the addition of cross-sectional detail. Although decubitus CTM has less spatial and temporal resolution compared with fluoroscopic techniques, cross-sectional information can be invaluable to detect otherwise occult CVFs, such as those involving the IVVP or veins superimposed with meningeal diverticula on an AP view. Furthermore, decubitus CTM may be superior in patients with a high body mass index, in whom fluoroscopic techniques are suboptimal secondary to poor x-ray penetration. Last, CTM in both the right and left lateral decubitus positions can usually be performed in a single day, obtaining diagnostic quality images by using only 10 mL total (5 mL per side) Omnipaque 300 or equivalent contrast agent (Fig 4).[40] The precise yield of decubitus CTM varies widely in the literature, even when stratified by pre-myelographic brain MR findings, and this is potentially due to differences in patient populations.[7,34] At least 1 study has directly compared DSM with decubitus CTM in the same patient population, demonstrating a higher diagnostic yield on decubitus CTM.[41]
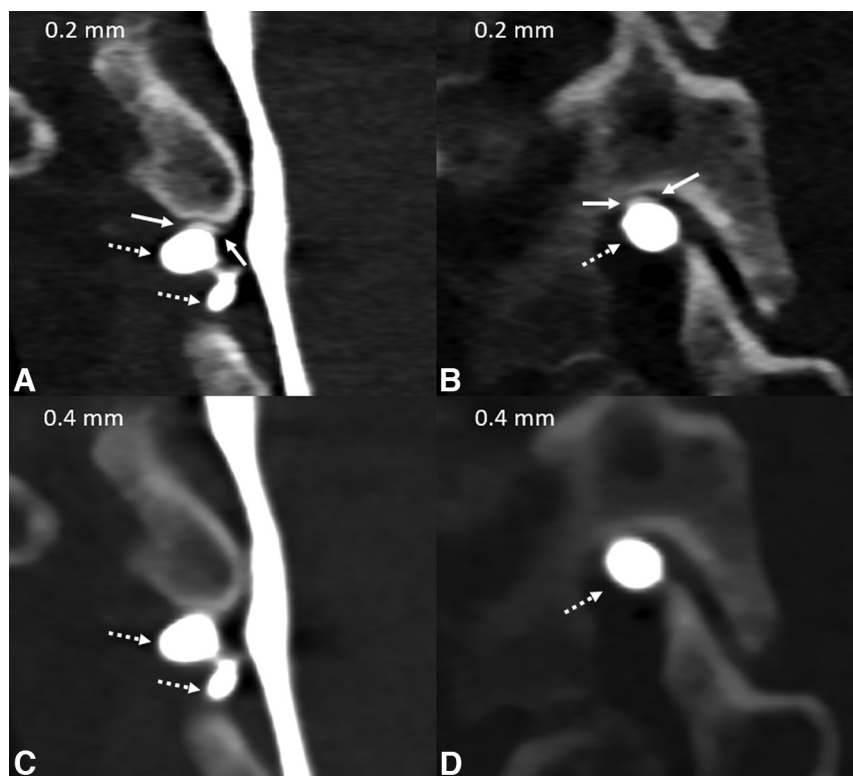
FIG 5. Advantage of high spatial resolution on PC-CTM for detection of a subtle CVF. Coronal and sagittal T3D 0.2 mm images (*A and B*) demonstrate a curvilinear opacification involving the right T2 intervertebral vein (*A and B, solid arrows*), clearly separate from the contrast-filled meningeal diverticulum (*A–D, dashed arrows*). The fistula is not visible when the images are reconstructed at 0.4 mm, because the spatial resolution is insufficient to discriminate the vein from the meningeal diverticulum. In some cases, high spatial resolution is necessary to confidently visualize subtle CVFs, particularly those adjacent to other high-attenuation structures.

Photon-Counting Detector CT Myelography

Decubitus CTM was initially performed by using traditional EID CT scanners. More recently, the use of photon-counting detector CT (PCCT) for CVF detection has been described.[42,43] PCCT is an emerging technology that uses a novel x-ray detection mechanism to directly convert incident photons into an electrical signal with proportional energy. This is different from the mechanism of EID CT, which relies on a 2-step process wherein individual photon energy information is lost. Furthermore, PCCT detectors do not require physical septa between detector elements, which increases spatial resolution.[44]

Decubitus PC-CTM, recently having been shown to have a high diagnostic yield for CVF detection, has numerous advantages.[45] Perhaps the most important of these is that substantially higher spatial resolution can be achieved. The currently clinically available PCCT scanner (NAEOTOM Alpha, Siemens) has 2 scan modes: the ultra-high resolution (UHR) mode provides 0.2 mm section thickness images, whereas the standard resolution (SR) mode is limited to 0.4 mm thickness images. By comparison, most modern EID CT scanners have a minimum section thickness of 0.6 mm. The main trade-off between the UHR and SR PCCT scan modes is scan speed, with the SR mode typically scanning the spine twice as quickly. High spatial resolution is instrumental for detection of CVFs, often making them more conspicuous or revealing otherwise occult lesions. This is because the veins draining CVFs are usually small in caliber and can be immediately adjacent to high attenuation structures such as the vertebral elements or contrast-opacified meningeal diverticula (Fig 4 and Fig 5). Furthermore, thin contrast columns within larger veins are better seen with high spatial resolution. As with EID CT, sharp kernel reconstructions can also help increase spatial resolution. This can result in substantial image noise, but denoising algorithms can be used to retain an acceptable SNR (Fig 6).[38]

Another potential advantage of PC-CTM is its inherent spectral sensitivity, which is a function of incident photons being binned into different energy ranges. This has 2 key benefits for the detection of CVFs. First, a low-energy threshold reconstruction (referred to as "T3D" by the manufacturer) is used to remove contribution from photons with an energy less than 20–25 keV. These low-energy photons typically represent electronic noise. Thus, the T3D reconstruction has improved SNR. Second, low kiloelectron volt VMIs can be created to maximize iodine conspicuity. Modern dual-energy CT can provide similar images, but this typically comes at the cost of slower scan speeds and/or increased radiation dose. By contrast, the spectral information needed to create VMIs is obtained automatically with PCCT, obviating the need for separate scan modes and retaining scan speed. In our practice, each scan obtained during PC-CTM is reconstructed with a 40 keV VMI and separately with a low-energy threshold (T3D), maximizing the advantages of both to detect CVFs (Fig 7).[45]

Finally, PC-CTM has higher temporal resolution than decubitus CTM on EID scanners, although the difference between the two is dependent on the specific EID scanner and protocol used. In our experience, the UHR mode of PC-CTM scans the entire spine in approximately 10–12 seconds (depending on patient size), while the SR scan mode does the same in 5–6 seconds. At our institution, this compares with an average of 20–25 seconds per scan on EID CTM. When decubitus PC-CTM is performed in a dynamic fashion, which is our institutional preference, this high temporal resolution is helpful (Fig 7).

Intrathecal Gadolinium MR Myelography

GdM refers to T1-weighted spinal MR imaging performed after the instillation of intrathecal gadolinium.[46] Imaging of the entire spine can be performed in an early and/or delayed fashion, usually in the supine or prone position. Precise MR imaging protocols vary, with 3D T1-weighted spoiled gradient-recalled echo
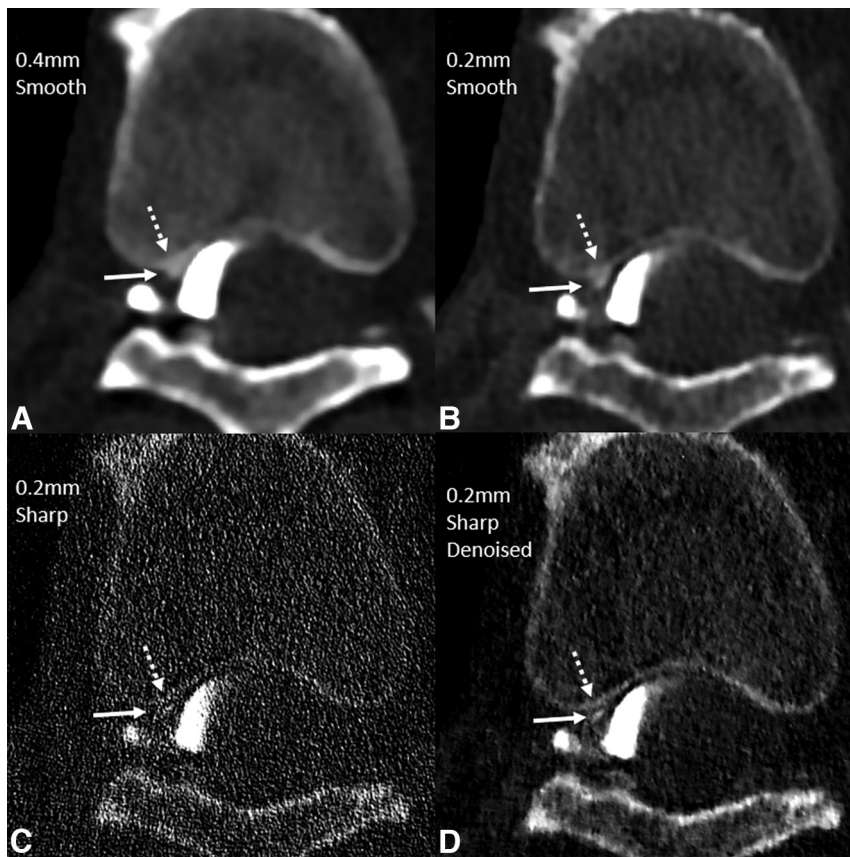
FIG 6. Benefit of high spatial resolution with a sharp kernel reconstruction and denoising to detect a subtle right T8 internal epidural CVF on PC-CTM. Four images from a right lateral decubitus PC-CTM are shown, all at the same section, timepoint, and window/level setting. Images were reconstructed at 0.4 mm with a smooth Br56 kernel (*A*), 0.2 mm with a smooth Br56 kernel (*B*), 0.2 mm with a sharp Qr89 kernel (*C*), and 0.2 mm with a sharp Qr89 kernel and denoising (*D*). A subtle CVF involving the ventral internal epidural venous plexus (*A–D, solid arrows*) is best seen and distinguished from the posterior vertebral body cortex (*A–D, dashed arrows*) on the denoised 0.2 mm sharp Qr89 kernel image.

sequences used at our institution.[46] In some cases, iodinated contrast may be injected as well to allow for a concurrent CTM. Although the use of GdM was initially described to localize slow leaks from meningeal diverticula, GdM can also detect CVFs (Fig 8).[47] The main advantage of GdM is the lack of ionizing radiation. Notable disadvantages include the relatively low spatial resolution, flow artifacts causing potential false-positive findings, and the inherent delay in imaging, which likely precludes detection of some quickly and transiently opacifying CVFs.[8] Furthermore, the use of intrathecal gadolinium is off-label, and care must be taken to inject only a small dose of gadolinium (usually no more than 0.5 mL, depending on the specific agent used) to avoid seizure and other life-threatening complications.

One study on GdM showed that it had a yield of 14% for the detection of CSF leaks, with a subset of the leaks found in that study being CVFs.[48] This is generally lower than most reported yields for CVF detection with other techniques, although no studies have directly compared GdM to other modalities. Nonetheless, some studies have demonstrated GdM's value in localizing CVFs.[47] Ultimately, more data are needed to understand if GdM should ever be used in patients with suspected

CVFs. We no longer perform GdM in patients with suspected CVFs unless all other modalities have been unrevealing.

PROVOCATIVE MANEUVERS TO AID IN CVF DETECTION

Despite the many and improving imaging modalities available to localize CVFs, these leaks sometimes remain occult, and patients may be subjected to multiple myelographic studies as a result. In recent years, various maneuvers have been used to improve CVF detection. First, it is important to optimize patient positioning. As previously noted, performing myelography in the decubitus position is known to increase the yield for CVF detection and is now considered essential.[30] In our experience, it is also helpful to elevate the patient's head while in the Trendelenburg position to minimize intracranial flow of contrast and maximize contrast volume in the nerve root sleeves. If a thoracic or cervical CVF is not found on initial imaging, performing lumbosacral myelography in the reverse Trendelenburg decubitus position may be helpful to exclude the rare lumbar or sacral CVF.[19] Second, specific respiratory maneuvers can be used to improve CVF conspicuity. Initially, it was shown that imaging during inspiration can make CVFs more visible, presumably by providing a higher pressure gradient between the intrathecal and venous compartments.[49] Subsequently, a technique termed "resisted inspiration" was shown to improve this pressure gradient even more, and several cases demonstrating the utility of this technique have since been published (Fig 9).[50,51] While precise technique varies, resisted inspiration typically involves forceful inspiration through a narrow apparatus, such as a Luer Lock syringe or a narrow straw. We usually instruct patients to forcefully inhale through a syringe for as long as possible during imaging. Importantly, resisted inspiration cannot be utilized if general anesthesia is used, as is sometimes done with DSM. A third technique that may improve CVF conspicuity is positive pressurization of the thecal sac, which is usually accomplished by injecting a variable amount of intrathecal saline immediately before myelography.[52] Although further study is needed to determine the incremental value of saline pressure augmentation, it poses relatively little risk and is commonplace at many institutions. One caveat is that intrathecal saline injection can create more turbulent intrathecal flow, which can impair layering of high-attenuation contrast.

Finally, 1 theoretic method to increase CVF conspicuity and potential area of future research would be selectively
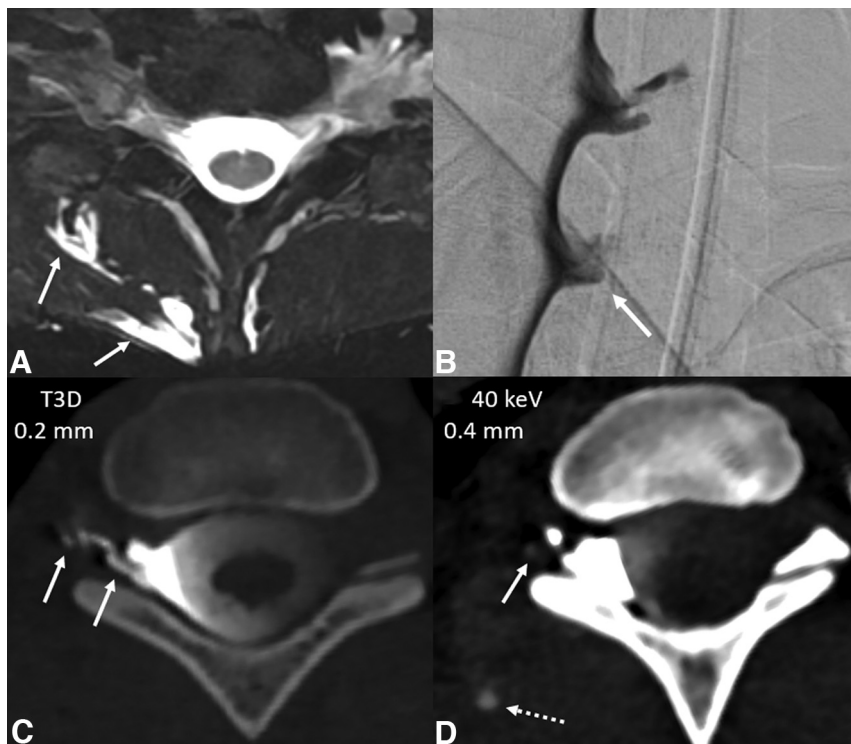
FIG 7. Right T1 CVF associated with a paraspinal venous malformation, demonstrating the complementary benefits of high spatial resolution, 40 keV VMIs, and high temporal resolution on PC-CTM. Axial T2-weighted MR imaging demonstrates a T2 hyperintense venous malformation (*A, solid arrows*), which extended from C7–T2. Right lateral decubitus DSM shows a small right T1 meningeal diverticulum (*B, solid arrow*), but no evidence of adjacent venous opacification. Right lateral decubitus PC-CTM was performed next. Axial 0.2 mm T3D (*C*) from this PC-CTM demonstrates a right T1 CVF (*C, solid arrows*). A 0.4 mm 40 keV (*D*) image obtained 8 seconds later shows that the vein has washed away (*D, solid arrow*), with new subtle opacification of the venous malformation (*D, dashed arrow*). 40 keV images are especially helpful for detecting subtle areas of contrast opacification such as this.
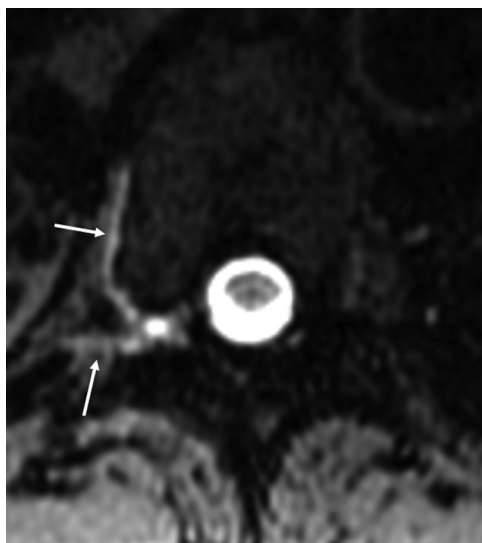

FIG 8. T1-weighted image from an GdM demonstrating a right T7 CVF involving the paraspinal segmental vein and lateral branches (*arrows*).

reducing central venous pressure before myelography. Although this has not been attempted to our knowledge, at least 1 case report describes a patient with SIH in the setting of bilateral common iliac vein thrombosis. It was thought that this patient had chronically reduced central venous pressure, leading to the development of a CVF. This patient's SIH dramatically improved after common iliac venous stent placement and short-term anticoagulation, corroborating the notion that low venous pressure increases flow through CVFs.[53] Future work investigating ways to selectively reduce central venous pressure may be helpful to increase the sensitivity of myelography for detecting CVFs in particularly challenging cases, but this remains speculative and requires further study.

CONCLUSIONS

CVFs are a common and increasingly recognized cause of SIH. As with all types of spinal CSF leak, detection and precise localization of CVFs are critical to permit targeted treatment, which may include surgery, transvenous Onyx (Medtronic) embolization, or percutaneous fibrin glue injection.[54,55] Here, we have summarized the currently available imaging modalities that can be used in CVF detection, namely conventional CTM, dynamic myelography, DSM, CB-CTM, EID CTM (with or without a dynamic component), PC-CTM, and GdM (Table). Given that only a subset of these modalities is available to most practicing radiologists, it is important to be familiar with each, as well as their advantages and disadvantages. Currently, the modalities with the highest reported yields in the literature are decubitus DSM, CTM, and PC-CTM.[31,34,45] Direct comparisons of these modalities are lacking, although decubitus CTM had a higher yield than DSM when both examinations were performed in 1 specific study population.[41] As knowledge and understanding of appropriate imaging techniques for CVF detection are further disseminated, multi-institutional collaboration and additional direct comparisons of different modalities will be more feasible.

Those performing myelography in patients with suspected CVFs should also be familiar with adjunctive patient-specific maneuvers. Decubitus positioning is essential in virtually all cases, and visualization of CVFs may be enhanced with techniques such as resisted inspiration and intrathecal pressure augmentation. Lowering the central venous pressure before myelography would theoretically also be helpful, and this may be a potentially fruitful area of further study. Finally, though not well-documented in the literature, it is the authors' opinion that some CVFs may be intermittent in nature, based on factors that are not understood and therefore cannot be controlled for. Thus, even if high-quality myelography is initially unrevealing,
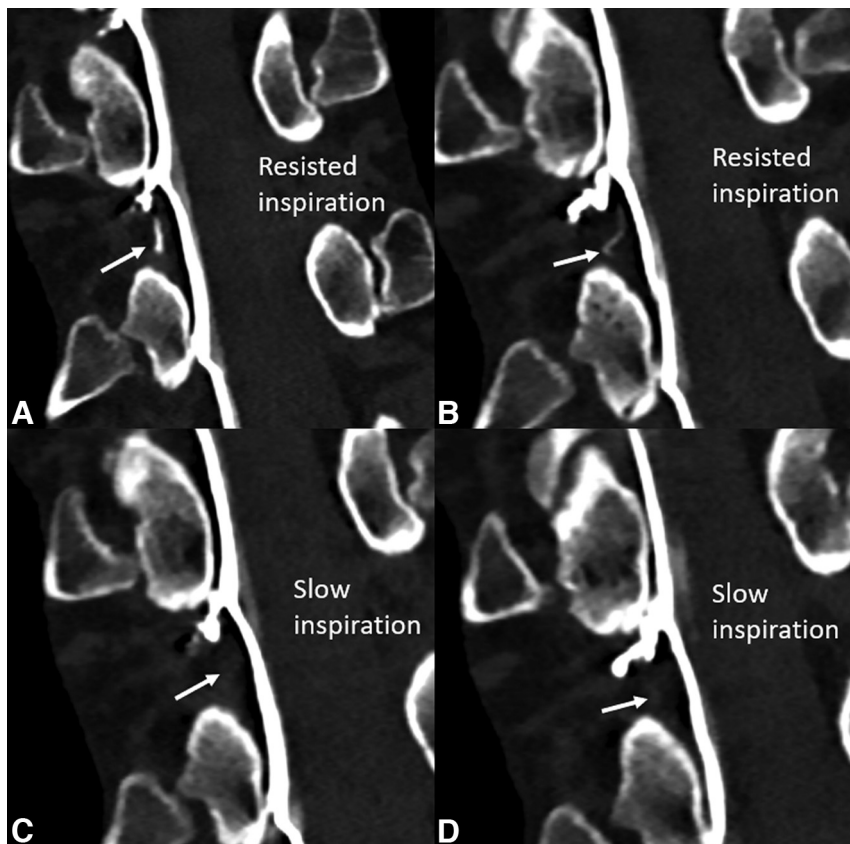
FIG 9. Benefit of resisted inspiration for the detection of a subtle right T11 CVF. Adjacent coronal images from a right lateral decubitus PC-CTM at 2 different time points (*A and B* versus *C and D*) obtained with resisted inspiration through a narrow syringe (*A and B*) and during slow inspiration through the mouth and nose (*C and D*) are shown. A clear right T11 CVF involving the internal epidural venous plexus is apparent during resisted inspiration (*A and B, arrows*) and completely occult during slow inspiration (*C and D*).

it is not unreasonable to repeat these studies at a later time if there is a high clinical suspicion for CVF.

Disclosure forms provided by the authors are available with the full text and PDF of this article at www.ajnr.org.

REFERENCES

1. Schievink WI, Maya MM, Jean-Pierre S, et al. **A classification system of spontaneous spinal CSF leaks.** *Neurology* 2016;87:673–79 CrossRef Medline

2. Liaw V, McCreary M, Friedman DI. **Quality of life in patients with confirmed and suspected spinal CSF leaks.** *Neurology* 2023;101: e2411–22 CrossRef Medline

3. Dobrocky T, Grunder L, Breiding PS, et al. **Assessing spinal cerebrospinal fluid leaks in spontaneous intracranial hypotension with a scoring system based on brain magnetic resonance imaging findings.** *JAMA Neurol* 2019;76:580–87 CrossRef Medline

4. Benson JC, Madhavan AA, Mark IT, et al. **Likelihood of discovering a CSF leak based on intracranial MRI findings in patients without a spinal longitudinal extradural collection: a new probabilistic scoring system.** *AJNR Am J Neuroradiol* 2023;44:1339–44 CrossRef Medline

5. Schievink WI, Maya M, Prasad RS, et al. **Spontaneous spinal cerebrospinal fluid-venous fistulas in patients with orthostatic headaches and normal conventional brain and spine imaging.** *Headache* 2021;61:387–91 CrossRef Medline

6. Farnsworth PJ, Madhavan AA, Verdoorn JT, et al. **Spontaneous intracranial hypotension: updates from diagnosis to treatment.** *Neuroradiology* 2023;65:233–43 CrossRef Medline

7. Kranz PG, Gray L, Amrhein TJ. **Decubitus CT myelography for detecting subtle CSF leaks in spontaneous intracranial hypotension.** *AJNR Am J Neuroradiol* 2019;40:754–56 CrossRef Medline

8. Mamlouk MD, Shen PY. **Myelographic timing matters.** *AJNR Am J Neuroradiol* 2023;44:E16 CrossRef Medline

9. Mark I, Madhavan A, Oien M, et al. **Temporal characteristics of CSF-venous fistulas on digital subtraction myelography.** *AJNR Am J Neuroradiol* 2023;44:492–95 CrossRef Medline

10. Schievink WI, Moser FG, Maya MM. **CSF-venous fistula in spontaneous intracranial hypotension.** *Neurology* 2014;83:472–73 CrossRef Medline

11. Callen AL, Timpone VM, Schwertner A, et al. **Algorithmic multimodality approach to diagnosis and treatment of spinal CSF leak and venous fistula in patients with spontaneous intracranial hypertension.** *AJR Am J Roentgenol* 2022;219:292–301 CrossRef Medline

12. Kranz PG, Gray L, Malinzak MD, et al. **CSF-venous fistulas: anatomy and diagnostic imaging.** *AJR Am J Roentgenol* 2021;217:1418–29 CrossRef Medline

13. Madhavan AA, Cutsforth-Gregory JK, Oushy SH, et al. **Combined CSF-venous fistula and middle meningeal artery embolization for treatment of spontaneous intracranial hypotension.** *Interv Neuroradiol* June 17, 2022. [Epub ahead of print] CrossRef Medline

14. Schievink WI, Maya MM, Moser F, et al. **Multiple spinal CSF leaks in spontaneous intracranial hypotension: do they exist?** *Neurol Clin Pract* 2021;11:e691–97 CrossRef

15. Madhavan AA, Benson JC, Cutsforth-Gregory JK, et al. **Co-existing fast CSF leaks and CSF-venous fistulas on dynamic CT myelography.** *Radiology Case Rep* 2022;17:2968–71 CrossRef Medline

16. Mamlouk MD, Shen PY, Jun P, et al. **Spontaneous spinal CSF leaks stratified by age, body mass index, and spinal level.** *AJNR Am J Neuroradiol* 2022;43:1068–72 CrossRef Medline

17. Kranz PG, Amrhein TJ, Gray L. **CSF venous fistulas in spontaneous intracranial hypotension: imaging characteristics on dynamic and CT myelography.** *AJR Am J Roentgenol* 2017;209:1360–66 CrossRef Medline

18. Pradeep A, Madhavan AA, Brinjikji W, et al. **Incidence of spontaneous intracranial hypotension in Olmsted County, Minnesota: 2019-2021.** *Interv Neuroradiol* March 22, 2023 [Epub ahead of print]. CrossRef Medline

19. Mark IT, Morris PP, Brinjikji W, et al. **Sacral CSF-venous fistulas and potential imaging techniques.** *AJNR Am J Neuroradiol* 2022;43:1824–26 CrossRef Medline

20. Simmons JK, Nadeem W, Maya MM, et al. **CSF-venous fistula of the clival skull base: a unique case study and literature review.** *Laryngoscope* 2023;134:645–47 CrossRef Medline

21. Madhavan AA, Kim DK, Brinjikji W, et al. **Diagnosis of a cerebrospinal fluid-venous fistula associated with a venous malformation using digital subtraction and computed tomography myelography.** *World Neurosurg* 2020;135:262–66 CrossRef Medline

22. Schievink WI, Maya MM, Moser FG, et al. **Spontaneous spinal CSF-venous fistulas associated with venous/venolymphatic vascular malformations: report of 3 cases.** *J Neurosurg Spine* 2019;32:305–10 CrossRef Medline

23. Madhavan AA, Kim DK, Carr CM, et al. **Association between Klippel-Trenaunay syndrome and spontaneous intracranial hypotension: a report of 4 patients.** *World Neurosurg* 2020;138:398–403 CrossRef Medline

24. Mokri B. **Klippel-Trenaunay-Weber syndrome (KTWS) and spontaneous spinal CSF leak: coincidence or link.** *Headache* 2014;54:726–31 CrossRef Medline

25. Soderlund KA, Mamlouk MD, Shah VN, et al. **Cerebrospinal fluid-lymphatic fistula causing spontaneous intracranial hypotension in a child with kaposiform lymphangiomatosis.** *Pediatr Radiology* 2021;51:2093–97 CrossRef Medline

26. Patel DM, Weinberg BD, Hoch MJ. **CT myelography: clinical indications and imaging findings.** *Radiographics* 2020;40:470–84 CrossRef Medline

27. Kranz PG, Amrhein TJ, Schievink WI, et al. **The "hyperdense paraspinal vein" sign: a marker of CSF-venous fistula.** *AJNR Am J Neuroradiol* 2016;37:1379–81 CrossRef Medline

28. Piechowiak EI, Pospieszny K, Haeni L, et al. **Role of conventional dynamic myelography for detection of high-flow cerebrospinal fluid leaks: optimizing the technique.** *Clin Neuroradiol* 2021;31:633–41 CrossRef Medline

29. Hoxworth JM, Trentman TL, Kotsenas AL, et al. **The role of digital subtraction myelography in the diagnosis and localization of spontaneous spinal CSF leaks.** *AJR Am J Roentgenol* 2012;199:649–53 CrossRef Medline

30. Schievink WI, Maya MM, Moser FG, et al. **Lateral decubitus digital subtraction myelography to identify spinal CSF-venous fistulas in spontaneous intracranial hypotension.** *J Neurosurg Spine* 2019;31:902–05 CrossRef Medline

31. Kim DK, Carr CM, Benson JC, et al. **Diagnostic yield of lateral decubitus digital subtraction myelogram stratified by brain MRI findings.** *Neurology* 2021;96:e1312–18 CrossRef Medline

32. Madhavan AA, Cutsforth-Gregory JK, Benson JC, et al. **Conebeam CT as an adjunct to digital subtraction myelography for detection of CSF-venous fistulas.** *AJNR Am J Neuroradiol* 2023;44:347–50 CrossRef Medline

33. Lützen N, Demerath T, Volz F, et al. **Cone-beam CT for the detection of a ventral spinal CSF leak in spontaneous intracranial hypotension.** *Neurology* 2023;101:670–71 CrossRef

34. Mamlouk MD, Ochi RP, Jun P, et al. **Decubitus CT myelography for CSF-venous fistulas: a procedural approach.** *AJNR Am J Neuroradiol* 2021;42:32–36 CrossRef Medline

35. Callen AL, Fakhri M, Timpone VM, et al. **Temporal characteristics of CSF venous fistulas on dynamic decubitus CT myelography: a retrospective multi-institution cohort study.** *AJNR Am J Neuroradiol* 2023;45:100–04 CrossRef Medline

36. Callen AL, Wojcik R, Bojanowski M. **A novel patient-positioning device for dynamic CT myelography.** *AJNR Am J Neuroradiol* 2023;44:1352–55 CrossRef Medline

37. Huynh TJ, Parizadeh D, Ahmed AK, et al. **Lateral decubitus dynamic CT myelography with real-time bolus tracking (dCTM-BT) for evaluation of CSF-venous fistulas: diagnostic yield stratified by brain imaging findings.** *AJNR Am J Neuroradiol* 2023;45:105–12 CrossRef Medline

38. Madhavan AA, Cutsforth-Gregory JK, Brinjikji W, et al. **Application of a denoising high-resolution deep convolutional neural network to improve conspicuity of CSF-venous fistulas on photon-counting CT myelography.** *AJNR Am J Neuroradiol* 2023;45:96–99 CrossRef Medline

39. Houk JL, Marin DM, Malinzak MD, et al. **Dual energy CT for the identification of CSF-venous fistulas and CSF leaks in spontaneous intracranial hypotension: report of four cases.** *Radiology Case Rep* 2022;17:1824–29 CrossRef Medline

40. Carlton Jones L, Goadsby PJ. **Same-day bilateral decubitus CT myelography for detecting CSF-venous fistulas in spontaneous intracranial hypotension.** *AJNR Am J Neuroradiol* 2022;43:645–48 CrossRef Medline

41. Lützen N, Demerath T, Würtemberger U, et al. **Direct comparison of digital subtraction myelography versus CT myelography in lateral decubitus position: evaluation of diagnostic yield for cerebrospinal fluid-venous fistulas.** *J Neurointerv Surg* November 2, 2023. [Epub ahead of print] CrossRef Medline

42. Madhavan AA, Yu L, Brinjikji W, et al. **Utility of photon-counting detector CT myelography for the detection of CSF-venous fistulas.** *AJNR Am J Neuroradiol* 2023;44:740–44 CrossRef Medline

43. Schwartz FR, Malinzak MD, Amrhein TJ. **Photon-counting computed tomography scan of a cerebrospinal fluid venous fistula.** *JAMA Neurol* 2022;79:628–29 CrossRef Medline

44. Sartoretti T, Wildberger JE, Flohr T, et al. **Photon-counting detector CT: early clinical experience review.** *Br J Radiology* 2023;96:20220544 CrossRef Medline

45. Madhavan AA, Cutsforth-Gregory JK, Brinjikji W, et al. **Diagnostic performance of decubitus photon-counting detector CT myelography for the detection of CSF-venous fistulas.** *AJNR Am J Neuroradiol* 2023;44:1445–50 CrossRef Medline

46. Akbar JJ, Luetmer PH, Schwartz KM, et al. **The role of MR myelography with intrathecal gadolinium in localization of spinal CSF leaks in patients with spontaneous intracranial hypotension.** *AJNR Am J Neuroradiol* 2012;33:535–40 CrossRef Medline

47. Chazen JL, Robbins MS, Strauss SB, et al. **MR myelography for the detection of CSF-venous fistulas.** *AJNR Am J Neuroradiol* 2020;41:938–40 CrossRef Medline

48. Madhavan AA, Carr CM, Benson JC, et al. **Diagnostic yield of intrathecal gadolinium MR myelography for CSF leak localization.** *Clin Neuroradiol* 2022;32:537–45 CrossRef Medline

49. Amrhein TJ, Gray L, Malinzak MD, Kranz PG. **Respiratory phase affects the conspicuity of CSF-venous fistulas in spontaneous intracranial hypotension.** *AJNR Am J Neuroradiol* 2020;41:1754–56 CrossRef

50. Mark IT, Amans MR, Shah VN, et al. **Resisted inspiration: a new technique to aid in the detection of CSF-venous fistulas.** *AJNR Am J Neuroradiol* 2022;43:1544–47 CrossRef Medline

51. Kranz PG, Malinzak MD, Gray L, et al. **Resisted inspiration improves visualization of CSF-venous fistulas in spontaneous intracranial hypotension.** *AJNR Am J Neuroradiol* 2023;44:994–98 CrossRef Medline

52. Callen AL, Pattee J, Thaker AA, et al. **Relationship of Bern score, spinal elastance, and opening pressure in patients with spontaneous intracranial hypotension.** *Neurology* 2023;100:e2237–46 CrossRef Medline

53. Kumar N, Neidert NB, Diehn FE, et al. **A novel etiology for craniospinal hypovolemia: a case of inferior vena cava obstruction.** *J Neurosurg Spine* 2018;29:452–55 CrossRef Medline

54. Brinjikji W, Madhavan A, Garza I, et al. **Clinical and imaging outcomes of 100 patients with cerebrospinal fluid-venous fistulas treated by transvenous embolization.** *J Neurointerv Surg* October 28, 2023. [Epub ahead of print] CrossRef Medline

55. Callen AL, Jones LC, Timpone VM, et al. **Factors predictive of treatment success in CT-guided fibrin occlusion of CSF-venous fistulas: a multicenter retrospective cross-sectional study.** *AJNR Am J Neuroradiol* 2023;44:1332–38 CrossRef Medline